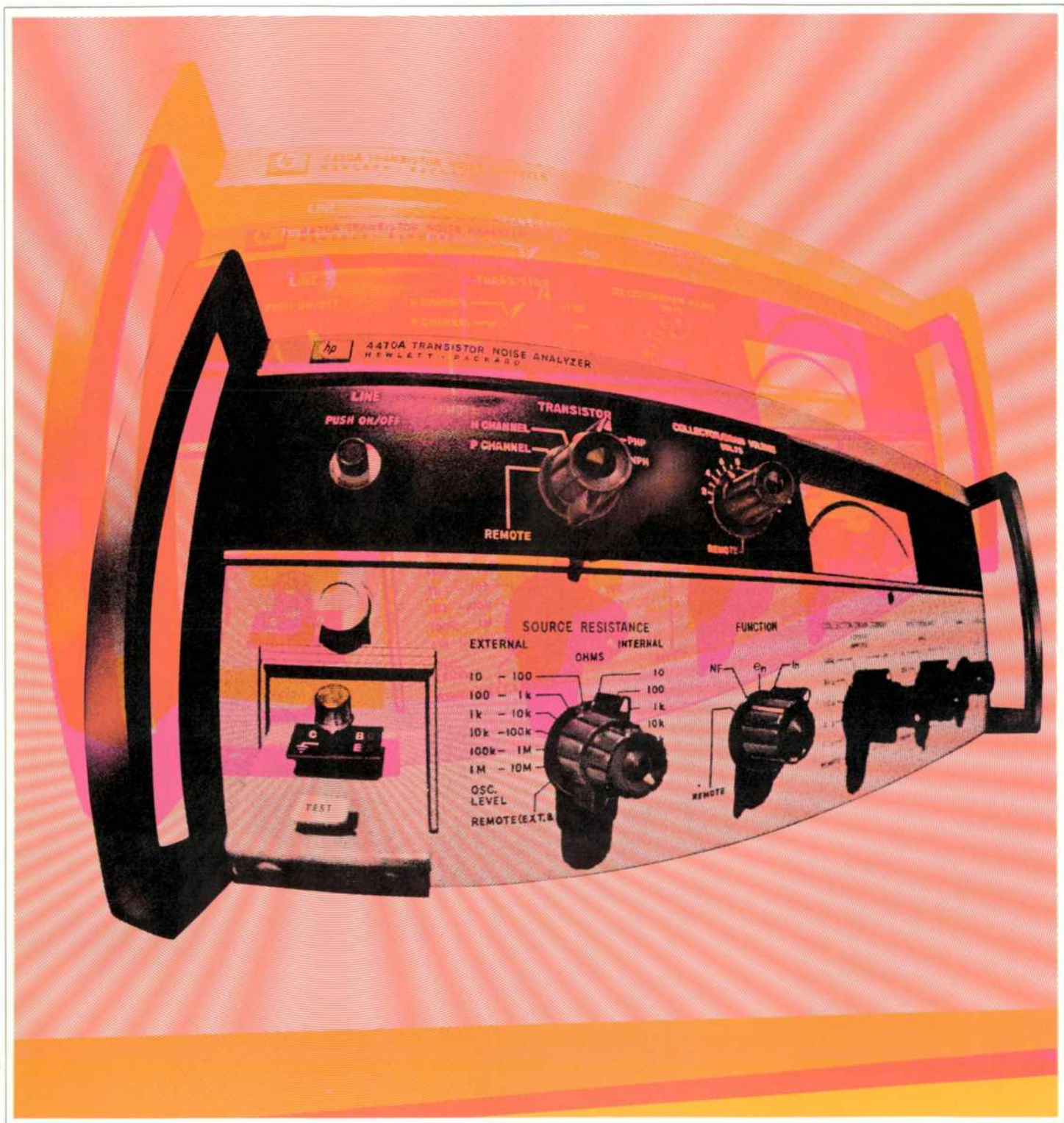


HEWLETT-PACKARD JOURNAL



OCTOBER 1969

Direct Measurement of Transistor Noise Voltage, Noise Current and Noise Figure

New analyzer measures noise in FET's and bipolar transistors from 10 Hz to 1 MHz. Rapid and easy operation makes it suitable for both lab and production testing.

By Haruo Itoh and Knud L. Knudsen

TRANSISTOR NOISE PERFORMANCE¹ is an important measure of transistor quality, and it determines the ability of the transistor to perform properly in critical applications. The internal noise sources in a linear twoport can be represented by two external noise sources connected to the input terminals—a voltage source e_n and a current source i_n .² From a small signal model which contains the internal noise sources, e_n and i_n can be calculated. However, for bipolar and field-effect transistors, not all internal sources can be readily determined from measurement of device parameters (see page 8). The excess noise, which increases with decreasing frequency, is difficult to predict. For bipolar transistors at low and intermediate emitter currents, the excess noise contributes primarily to i_n and increases with bias current. For FETs, it contributes mainly to e_n . For most practical source impedances, the i_n of FETs is insignificant.

In audio applications for example, excess noise can be annoying, and for measurement of slowly varying signals, it often becomes the dominant noise which sets the ultimate limit for the measurement accuracy. Variations in

the manufacturing process cause 1/f noise to vary among transistors, so for critical applications it becomes necessary to select low noise transistors. Often the selection becomes a matter of trying a transistor in a circuit, or predicting its noise performance by lengthy lab measurements and calculations. Now a rapid method of direct measurement of voltage noise, current noise and noise figure has been developed.

In a departure from traditional approaches, a new Hewlett-Packard instrument, the HP Model 4470A Transistor Noise Analyzer, measures the noise characteristics of bipolar and field effect transistors completely and accurately. (Previous techniques have relied on measurements of noise voltage and noise figure only.)

The new instrument, Fig. 1, measures directly e_n , i_n , and noise figure (NF) for bipolar transistors and e_n and NF for field effect transistors. Measurements are made at 4 Hz bandwidth at 11 spot frequencies between 10 Hz and 1 MHz. Three separate design achievements, each of some significance, that enable the Model 4470A to meet its measurement objectives are (1) an input circuit with low leakage and low stray capacitance for accurate measurement of all three noise parameters; (2) a phase lock and pilot signal detection technique that accurately controls overall system gain at the specific spot frequency of interest; and (3) a mixer circuit with bandpass filters to separate out the noise signal of interest at frequencies very close to the pilot frequency.

In evaluating the noise performance of a transistor the traditional approach is to use the noise figure value. Noise figure, however, gives only a value at a particular source impedance (see page 11). It is not possible to calculate either voltage noise or current noise from a noise figure value alone, nor is it possible to calculate NF at one source impedance from a given NF at a different source impedance.



Fig. 1. This new HP Model 4470A Transistor Noise Analyzer gives both noise voltage and noise current, resulting in a complete and accurate description of device noise performance. Appropriate meter scale units and multipliers are illuminated.

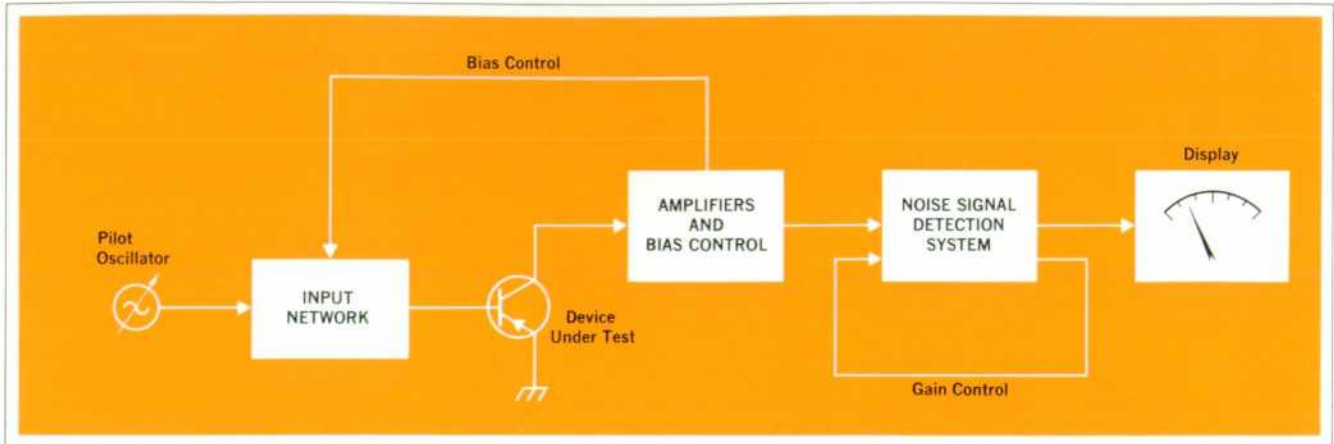


Fig. 2. In the Model 4470A, the input network provides the proper impedance for the measurement desired. Selection of source resistance for noise figure measurements is possible from 10 Ω to 10 M Ω internally or other values externally.

As shown in the basic block diagram, Fig. 2, a pilot signal at a selected spot frequency is applied to the device under test. The pilot signal is a reference so that constant overall system gain can be maintained regardless of the gain of the device under test. Biasing is controlled automatically to provide the selected collector/drain current and voltage values. Noise and pilot signal are separated by the noise detection system, and gain control is established by monitoring the level of the pilot signal. After separation, the noise signal is converted to dc and displayed on the front panel meter.

A transistor with all internal noise sources referred to the input as a voltage generator, e_n , and a current generator, i_n is shown in Fig. 3. For i_n measurement, the input to the transistor should be open circuited, and for measuring e_n , the transistor input should be shorted. NF de-

pends upon the value of source resistance selected. For NF measurements, the selected value of source resistance is connected across the transistor input.

In the actual measurement of transistor noise, the bias and pilot signals are applied to the transistor under test while approximating the required short or open circuit conditions.

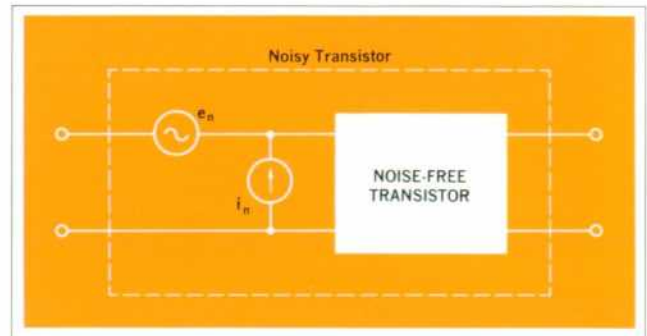


Fig. 3. A simplified transistor noise model consisting of voltage and current noise generators at the input of an 'ideal' noise-free transistor.

Cover: The Hewlett-Packard Model 4470A Transistor Noise Analyzer measures transistor noise voltage, noise current and noise figure directly from 10 Hz to 1 MHz. It is suited for laboratory and production. See page 2.

In this Issue:

Direct Measurement of Transistor Noise	page 2
Sources of Noise in Transistors.....	page 8
Electronic Monitor for Heartbeat Patterns	page 12
Electrical Performance of the Heart	page 14
Ectopic Beats.....	page 15

Measuring i_n

Fig. 4(a) represents the transistor noise model connected to the pilot signal source and bias supply. Y_s is the source admittance. $Y_s = g_s + j\omega C_s$ and i_{ns} is the thermal noise current from g_s .

Fig. 4(b) is the current equivalent of Fig. 4(a). $\overline{i_{ns}^2} =$

$4kT\Delta f g_s$. Two conditions must be met for accurate measurement of i_n :

- (1) $\overline{i_{ns}^2} \ll \overline{i_n^2}$
- (2) $|Y_s|^2 \overline{e_n^2} \ll \overline{i_n^2}$

In the Model 4470A, these conditions are met by circuit design innovations in two areas. First, the pilot signal is applied to the device under test through a very small (0.5 pf) input capacitance. An integrator between the pilot oscillator and the input capacitance compensates for the change in reactance of the input capacitor with changes in frequency. As a result, pilot signal level applied to the device under test is constant for all spot frequencies.

Secondly, bias current is supplied to the base of the device under test through 20 diodes in series with a 2 k Ω resistor. Then the $\overline{i_{ns}^2}$ of the bias input circuit is 1/20 the value of the theoretical minimum value for $\overline{i_n^2}$ of the device under test.

Unusual measures were taken in mechanical design and choice of proper materials so that the input circuitry has very small leakage conductance and very low stray capacitance.

Design of the input and bias circuits assures that the two required conditions for accurate measurement are met for all specified values of i_n .

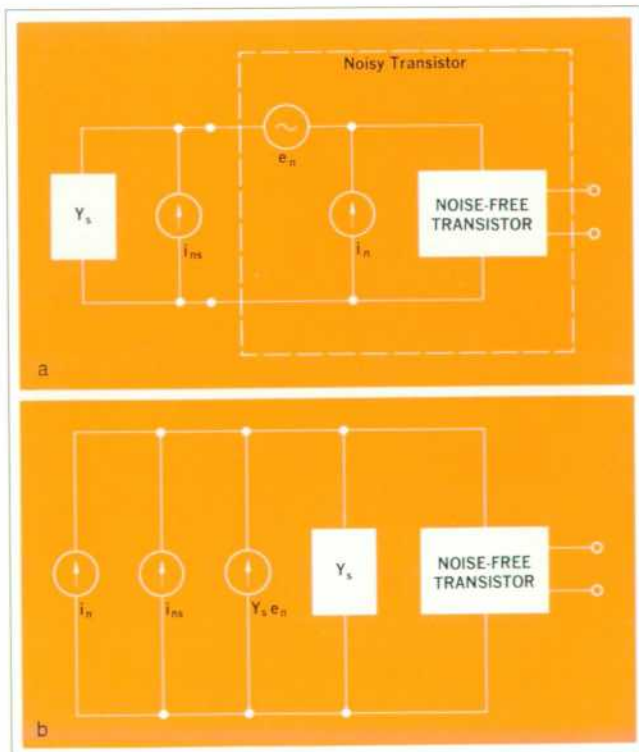


Fig. 4. Transistor noise model for i_n measurement (a), and its current equivalent (b).

Measuring e_n

Fig. 5(a) shows the transistor noise model connected to the pilot signal source and bias supply for e_n measurement. Z_s is the source impedance. $Z_s = r_s + \frac{1}{j\omega C}$ and e_{ns} is the thermal noise voltage from r_s .

Fig. 5(b) is the voltage equivalent of Fig. 5(a), and $\overline{e_{ns}^2} = 4kT\Delta f r_s$.

Two conditions must be met for accurate measurement of e_n :

- (1) $\overline{e_{ns}^2} \ll \overline{e_n^2}$
- (2) $|Z_s|^2 \overline{i_n^2} \ll \overline{e_n^2}$

These conditions are met by supplying the pilot signal across a 1 Ω input resistor in series with 6000 μ F. At 10 Hz, the worst case, the absolute value of Z_s is less than 2.9 Ω , which amply meets the conditions for accurate e_n measurements.

For noise figure (NF) measurements, the pilot signal and bias are supplied to the device under test through the selected source resistance.

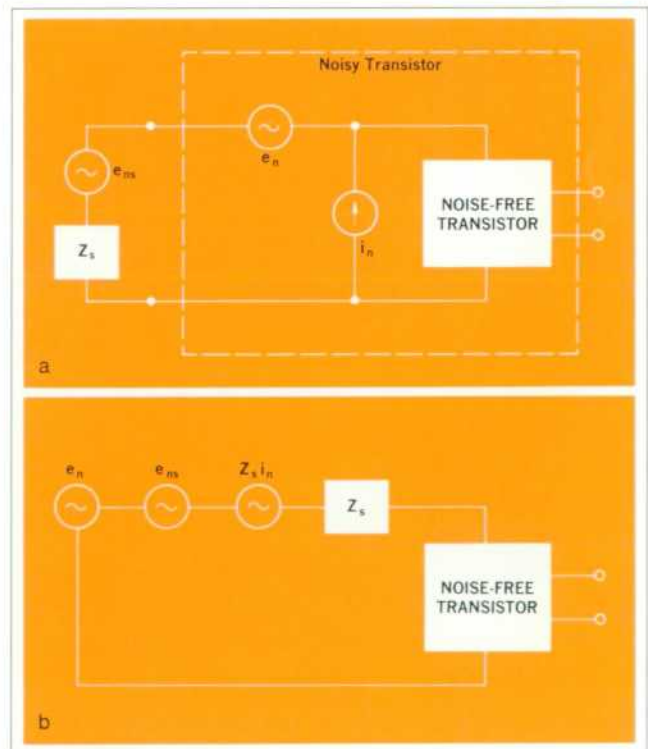


Fig. 5. Transistor noise model for e_n measurement (a), and its voltage equivalent (b).

Keeping Gain Constant

Transistor noise measurements include the transistor itself as an active amplifying element. Since the transistor's gain is unknown, an automatic gain control technique is used to normalize overall system gain to a fixed value independent of the transistor being tested.

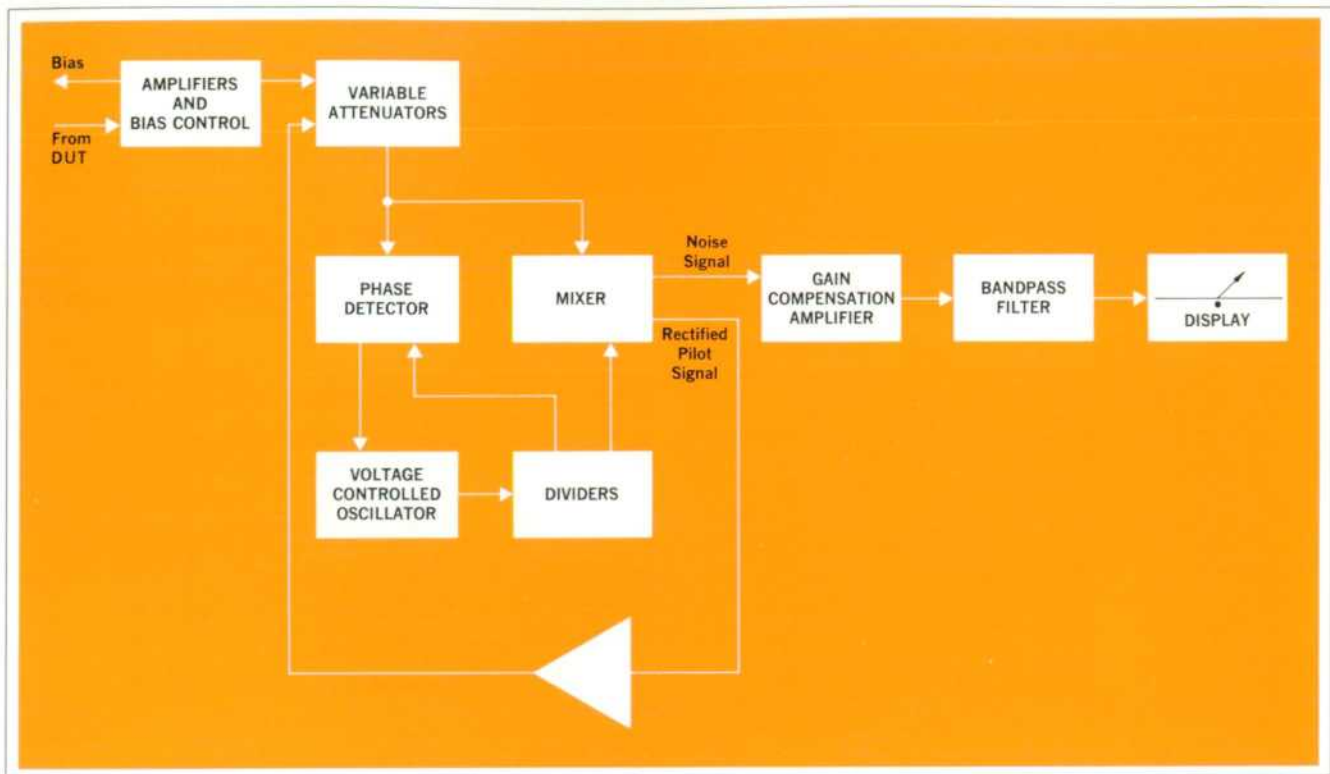


Fig. 6. Noise signal detection system uses a phase lock technique to maintain constant gain regardless of the gain of the device under test.

The Model 4470A uses phase lock, Fig. 6, to maintain constant overall system gain at whatever spot frequency transistor noise is being measured.

The output of the voltage-controlled oscillator, which operates at 4 times the selected pilot frequency, is fed to a divider circuit. This in turn produces four square waves having the same frequency as the pilot. One of the square waves is in phase with the pilot and another is 180° out of phase with the pilot. These two square waves go to the mixer input.

A third square wave leads the pilot by 90° , and the fourth lags the pilot by 90° . These two square waves go to the phase detector, which delivers an error signal to the voltage-controlled oscillator if the two square waves are not exactly 90° out of phase with the pilot.

The two square waves fed to the mixer mix with the combined pilot and noise signal producing a dc signal proportional to pilot signal amplitude. This dc signal is fed back to the variable attenuators to maintain constant system gain regardless of the gain of the device under test.

The Model 4470A measures noise in two 4 Hz wide bands centered 10 Hz above and below the pilot frequency. The action of the mixer translates these two narrow bands to a center frequency of 10 Hz. Passing the mixer output noise signal through a bandpass filter

with 10 Hz center frequency removes other noise frequencies, and passes to the display section the noise signal contained in the two bands above and below pilot frequency.

Acknowledgments

The Transistor Noise Analyzer design was the result of a study conducted at HP Laboratories under supervision of Paul E. Stoft. Bas Hoeks and Knud Knudsen, both of HPL, defined and solved the fundamental problems and built the first working model.

The authors wish especially to acknowledge the contributions of the following: Nobuo Numasaki, now YHP engineering manager, who designed the phase lock system and display logic; Masahide Nishida, Transistor Noise Analyzer project leader from March 1968 to March 1969 and now product manager for the TNA; Takayuki Sato did the amplifiers and filtering and was project leader to the conclusion of the project; Kazunori Shibata who handled the industrial design phase of the project; Toshio Manabe who did the mechanical design of the TNA. Other contributors at YHP include Hiroshi Mimura, Yoshiaki Okuyama and Kenichi Abiko.

Special thanks for important contributions go to Bob Dudley and Ron Tuttle of the HP Loveland Division. 

Reference

1. Michael C. Swiontek and Rolly Hassun, 'The Influence of Transistor Parameters on Transistor Noise Performance,' Hewlett-Packard Journal, Vol. 16, No. 7, March 1965, page 8.
2. H. A. Haus, et al, 'Representation of Noise in Linear Twoports,' Proc. IEEE, Vol. 48, pp. 69-74, January 1960.



Haruo Itoh

Haruo Itoh received his BSEE from Tokyo Institute of Technology in 1959. He then joined Yokogawa Electric Works as an R & D engineer. While with Yokogawa he worked on ac and dc millivoltmeters, on an RF millivoltmeter and on a clip-on ammeter.

Haruo joined YHP in 1964 and worked on a vibrating reed electrometer and on the design of the Model 4260A Impedance Bridge. He contributed to the article on the impedance

bridge in the September 1966 issue of the Hewlett-Packard Journal.

Haruo developed the input circuitry for the 4470A. He is presently engaged in investigation of new product areas for YHP.



Knud L. Knudsen

Knud Knudsen received his degree in electrical engineering from Aarhus Elektroteknikum, Aarhus, Denmark in 1957.

Before joining HP in 1963, Knud spent 6 years with the Radio Receiver Research Laboratory of the Academy of Technical Sciences, Copenhagen. At Hewlett-Packard Laboratories, he has worked on measurement of noise in transistors, low-noise circuits, parametric amplification and on circuit design on various

projects.

Knud is an Associate Member of IEEE. He plays tennis, skis, and enjoys classical music.

SPECIFICATIONS

HP Model 4470A

Transistor Noise Analyzer

NOISE PARAMETERS MEASURED:

VOLTAGE NOISE: (e_n) referred to the input of the transistor under test, in bipolar and field-effect transistors.

CURRENT NOISE: (i_n) referred to input of transistor under test, in bipolar transistors.

SPOT NOISE FIGURE: (NF) for both bipolar and field-effect transistors.

AVAILABLE RANGES:

VOLTAGE NOISE: Full-scale values of 3 nV, 10 nV, 30 nV, 100 nV, 300 nV, 1000 nV and 3 μ V at 1 Hz bandwidth are provided. Two meter scales (0 to 3, 0 to 10), and X1, X10, and X100 multipliers are used.

CURRENT NOISE: Noise current measurement is a function of collector/drain current and ranges from 100 fA to 3 nA.

SPOT NOISE FIGURE: (NF) 0-40 dB; meter scaled from -5 dB to +10 dB.

Ranges are: -5 dB to +10 dB

+5 dB to +20 dB

+15 dB to +30 dB

+25 dB to +40 dB

SPOT FREQUENCIES: 10 Hz, 30 Hz, 100 Hz, 300 Hz, 1 kHz, 3 kHz, 10 kHz, 30 kHz, 100 kHz, 300 kHz, and 1 MHz.

NOISE BANDWIDTH: 4 Hz, equivalent noise bandwidth.

COLLECTOR/DRAIN POWER SUPPLIES:

Collector/Drain currents of 1, 3, 10, 30, 100 μ A, 0.3, 1, 3, 10, and 30 mA are provided; Vernier provides continuous adjustment between these values; Current monitoring output on rear panel. Collector/Drain Voltages of 0 to 15 Vdc, continuously variable at front panel, monitored at rear-panel jack. Both supplies are independently controlled, changes in one supply will not affect the other. The current is controlled by regulation of the base/gate bias. Current supply seeks desired setting irrespective of type of FET tested (i.e., MOSFET, etc.).

ACCURACIES:

COLLECTOR/DRAIN VOLTAGES:

$\pm 3\%$ at monitor jack; $\pm 10\%$ at front panel.

COLLECTOR/DRAIN CURRENT:

$\pm 3\%$ at monitor jack; $\pm 3\%$ at calibrated front panel setting.

SPOT FREQUENCY: $\pm 3\%$.

NOISE BANDWIDTH: $\pm 3\%$.

TOTAL MEASUREMENT ACCURACY: Determined by above plus accuracy of internal circuitry plus averaging of meter or analog output. Better than ± 1 dB.

TRANSISTOR TYPES: Bipolar NPN and PNP, P-channel or N-channel FET noise may be analyzed.

β -RANGE: Bipolar Transistors from 10 to 1000 are measurable.

SOURCE RESISTANCE:

INTERNAL: Values provided for use when measuring Noise Figure are 10 Ω , 100 Ω , 1 k Ω , 10 k Ω , 100 k Ω and 1 M Ω . Other values from 10 to 10 M may be applied at EXT RES holder on front panel.

REMOTE PROGRAMMING: Seven front-panel functions may be remotely controlled by external contact closure between pins of rear-panel connectors. Programmable functions are FUNCTION, FREQUENCY, CURRENT, VOLTAGE, METER RANGE, SOURCE RESISTANCE, TRANSISTOR. (Pilot signal level, Collector/Drain current vernier are programmable by external resistance.)

TRANSISTOR BIAS/SUPPLY OUTPUTS: Available at three rear-panel BNC connectors for monitoring purposes are: Collector/Drain current, Collector/Drain Voltage Base/Gate Voltage.

RECORDER OUTPUT: Proportional to meter deflection, 0-1 Vdc, 1 k Ω output resistance. BNC Connector.

TRANSISTOR SOCKET CONFIGURATIONS:

Six modular sockets provided with different lead configurations.

POWER REQUIRED: 115/230 Vac, $\pm 10\%$, 50 or 60 Hz, 60 W.

WEIGHT: 32 lb (14.5 kg).

ACCESSORIES PROVIDED: Power cord, External resistor holder, (fitted with typical resistor), six modular sockets.

PRICE: \$4450.00.

MANUFACTURING DIVISION: YOKOGAWA-HEWLETT-PACKARD LTD.

9-1, Takakura-cho, Hachioji-shi
Tokyo, Japan

Sources of Noise in Transistors

By Niladri R. Mantena

THE MOST IMPORTANT NOISE SOURCES in semiconductors are thermal noise, shot noise, generation-recombination noise, and $1/f$ noise. Thermal noise, also called Johnson noise, is due to the random motion of charge carriers in the semiconductor. It is present whether or not an electric field is applied. The noise spectrum is flat up to the far-infrared frequencies. Its magnitude may be calculated from thermodynamical considerations so that its result is independent of the 'model' used in deriving the spectrum.

Shot noise, also known as Schottky noise, is caused by spontaneous fluctuations in the free carrier densities. In those semiconductor devices such as photoconductors and field-effect transistors in which the current flow is due to *carrier drift*, the local fluctuations in free carrier density are a result of fluctuations in the generation rates, recombination rates, trapping rates, etc., of the carriers. In those semiconductor devices such as diodes and bipolar transistors in which the current flow is also due to *carrier diffusion*, the fluctuations in free carrier density are modified by fluctuations in the diffusion process.

In bulk-effect devices the name generation-recombination noise is more appropriate than shot noise, since the carrier density fluctuations exist even if no electric field is applied; applying a field is only the most convenient way of detecting the fluctuations. Thus, the excess noise in a junction-gate field effect transistor (JFET) is mainly of the generation-recombination (g-r) type and is shown¹ to result from Shockley-Read-Hall centers in the transition region of the gate junction.

Junction devices, such as diodes and transistors, operate on the principle of minority carrier injection and an applied field is needed to produce or change the injection level. The generation-recombination noise in this case shows much closer resemblance to the field- or current-dependent shot noise than in the bulk-device case. The minority carriers in the base region of a bipolar transistor or in the very-thin channel region of an insulated gate field effect transistor (IGFET) are readily affected by the

slow trapping states at the surface of the device. The modern planar transistors are all passivated by silicon dioxide to reduce the surface effects. Detailed experiments on silicon/silicon dioxide interfaces² indicate that there is a certain amount of surface charge located within 200 Å of the oxide-silicon surface and that its magnitude is a function of the process used to grow the oxide.

The model postulated by McWhorter³ and used widely in flicker noise calculations⁴ assumes that the surface states act as traps and give rise to current carrier fluctuations in the device. It is further assumed that the free carriers at the oxide-silicon surface communicate with the surface states within the oxide by tunneling through the oxide barrier and that the tunneling mechanism provides a wide distribution of trapping times needed to give $1/f$ spectrum for the excess noise. Christensson et al¹ have shown that the largest contribution to $1/f$ noise in IGFETs comes from surface states near the quasi Fermi level of current carriers in the channel and that the magnitude of $1/f$ noise is proportional to the surface-state density. The analysis for excess noise voltage in JFETs and IGFETs are well covered in the literature by Sah¹ and Christensson et al¹, respectively. The remarkable feature of excess noise in FETs is its relative independence on the operating conditions of the transistor in distinct contrast with excess noise in bipolar transistors. The low-frequency (g-r type) excess noise in JFETs depends on the bulk material properties, i.e., number and occupation of traps and the majority carrier life time and can be reduced by careful design. The low-frequency ($1/f$ type) excess noise in IGFETs can be reduced by reducing the surface state density. The mean square thermal noise voltage in FETs is inversely proportional to the transconductance and can be modified by changing the operating drain current. Current noise in FETs is very small and their noise figure decreases with increasing source resistance in the frequency range where the device capacitances can be neglected.

Noise in Bipolar Transistors

The complete noise model of a bipolar transistor including thermal and shot noise sources was proposed by van der Ziel⁵ and Nielsen⁶. A complete description of the model, excluding the excess noise sources, and the magnitude and variation with operating point of the noise parameters were presented in graphic form by Swiontek and Hassun⁷. A general 1/f for flicker-noise model for bipolar transistors and its justification based on experiments were presented by Plumb and Chennette⁸. The complete noise equivalent circuit including the flicker noise sources and the expressions for all noise source terms for an NPN transistor are shown in Fig. 1. Here $\overline{e_{nb}^2}$ is the mean square Johnson noise voltage in the base spreading resistance r'_b , $\overline{i_{re}^2}$ is the shot noise in the emitter current, $\overline{i_{rc}^2}$ is the flicker noise due to the recombination of minority carriers (electrons) at the base surface region. The empirical expressions for $\overline{i_{rc}^2}$ is derived from Fonger's model⁹. C_f is an empirical constant that depends on the energy level, density, and the capture cross-section of the traps located at the base surface region. The flicker current noise $\overline{i_{rc}^2}$ of the collector junction is completely correlated to the emitter junction noise and is negligible by comparison. Thus, a low-frequency noise equivalent circuit for the noise parameters, e_n and i_n , of a common-emitter amplifier can be drawn as shown in Fig. 2. The complete expressions for e_n , i_n and the noise figure of

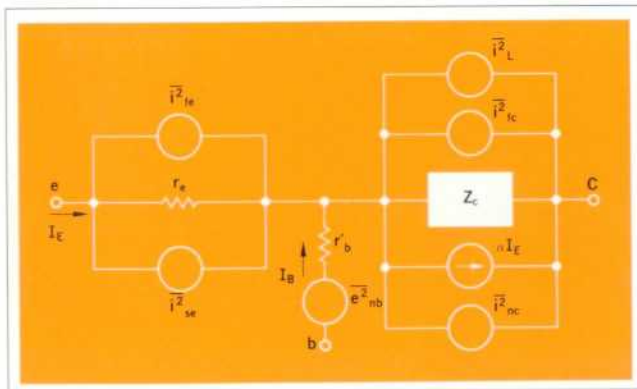


Fig. 1. Noise equivalent circuit including the flicker noise sources, where

$$\overline{e_{nb}^2} = 4kTB r'_b, \overline{i_{re}^2} = 2qBI_E = \frac{2kTB}{r_e}, \overline{i_{rc}^2} = 2q\alpha_c(1 - \alpha_c)I_E B + 2qBI_{co},$$

$\overline{i_{rc}^2}$ = Leakage current noise including its flicker component,

$\overline{i_{re}^2} = C_f h_{ie} \frac{I_B S}{f} B$ (emitter junction flicker noise based on Fonger's model), $\overline{i_{rc}^2}$ = Flicker noise current in the collector junction; and i_{rc} is completely correlated to i_{re} and

$$\frac{\overline{i_{rc}^2}}{\overline{i_{re}^2}} \gg 1.$$

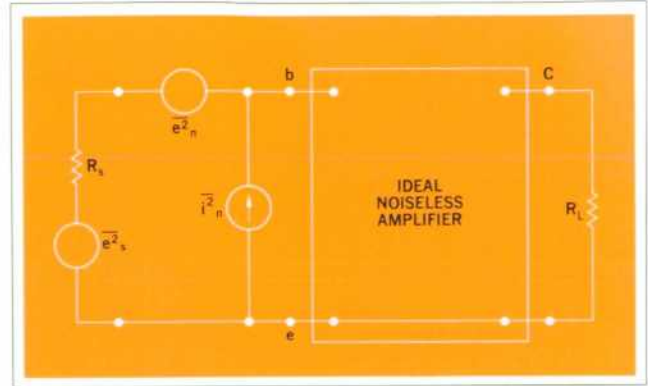


Fig. 2. e_n , i_n representation for common-emitter amplifier for low I_E such that $h_{ie} r_e \gg r'_b$, where

$$\overline{e_n^2} = 4kTB r'_b + \frac{2kTB}{r_e} + \overline{i_{n1}^2} r'_b{}^2 + \overline{i_{n2}^2} r_e{}^2 + 2\overline{i_{n1} i_{n2}} r'_b r_e \delta,$$

$$\overline{i_n^2} = \overline{i_{n1}^2} + \frac{\overline{i_{n2}^2}}{h_{ie}^2} + 2\delta \frac{\overline{i_{n1} i_{n2}}}{h_{ie}}, \overline{i_{n2}^2} = \overline{i_{nc}^2} + \overline{i_c^2} + \overline{i_{rc}^2}.$$

$$\overline{i_{n1}^2} = 2qBI_B + C_f \frac{I_B S}{f} B, \text{ and}$$

$$F = 1 + \frac{1}{4kTB} \left(\overline{i_n^2} R_s + \frac{\overline{e_n^2}}{R_s} + 2\gamma \overline{e_n i_n} \right); \gamma \text{ is the factor of}$$

cross correlation between e_n and i_n and has values between 0 and 1 depending upon the operating conditions.

the amplifier with a source resistance R_s are also given there. The parametric dependence of e_n , i_n and noise figure will be briefly discussed.

Noise Voltage e_n

The noise voltage of a bipolar transistor for high current gain (>100) can be completely specified by r'_b and r_e since the contributions of noise current sources i_{n1} and i_{n2} can be neglected by comparison with the voltage sources. A simplified expression for e_n may be written as:

$$\overline{e_n^2} = 4kTB \left(r'_b + \frac{r_e}{2} \right)$$

It can be seen that $\overline{e_n^2}$ is just the Johnson noise in r'_b at high currents where $r'_b \gg r_e$. At low currents where $\frac{r_e}{2} \gg r'_b$, the noise voltage may be expressed as

$$\overline{e_n^2} = 2kTB r_e = \frac{2(kT)^2 B}{qI_E}$$

Thus, at low currents, e_n varies as $(I_E)^{-1/2}$ and is independent of frequency as long as the flicker current noise is so small that its contribution to e_n can be neglected. These basic conclusions on e_n are well substantiated by the experimental results of e_n vs I_C for a low-current, high-gain, low-noise bipolar transistor shown in Fig. 3. It may be seen that e_n approaches $4nv/\sqrt{\text{Hz}}$ for $I_C > 100 \mu\text{A}$. The value of r'_b calculated from this asymptotic value of e_n is about 1000Ω and is in reasonable agreement with an independent measurement of r'_b . This value of r'_b is rather high because of the very lightly doped base

but its contribution to e_n at low collector currents is negligible compared to that of $r_e/2$.

Noise Current i_n

In general, the contributions to $\overline{i_n^2}$ from $\overline{i_{I_B}^2}$ and $\overline{i_{I_C}^2}$ are very small for devices with low leakage currents and large h_{FE} (> 100). Thus, to a good approximation, i_{n1} completely determines the input-referred current noise. The two components of $\overline{i_{n1}^2}$ are: 1) shot noise of the dc base current, and 2) the flicker noise current due to base surface recombination current. If the emitter junction is formed in a manner designed to yield very little surface damage and surface recombination, the flicker component of the current noise is small at low collector currents. The current noise spectra of a low-noise, high-gain device is shown in Fig. 4 for $I_C = 1 \mu\text{A}$ and $100 \mu\text{A}$ and show the $1/\sqrt{f}$ behavior for frequencies below 100 Hz. The corner frequency, where the mean square flicker noise equals the mean square shot noise, is about 50 Hz for $I_C = 1 \mu\text{A}$ and increases to about 300 Hz for $I_C = 100 \mu\text{A}$. The rapid increase of flicker noise current with increasing base current is shown in Fig. 5. While the shot noise current increases as $\sqrt{I_B}$, the flicker component itself increases as $(I_B)^l$, where l is 0.7 for low I_B (I_C) and unity for higher values of I_B and I_C . This explains the corner frequency increase with increasing collector (base) current and also indicates why it is desirable to operate bipolar transistors at as low a collector current as is consistent with the current gain and the circuit requirements. The flicker and shot noise currents vary as square root of collector current.

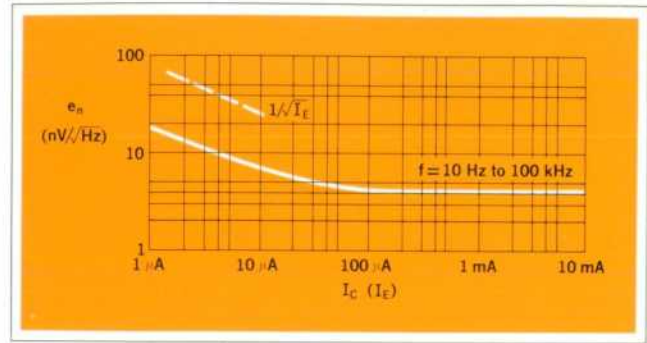


Fig. 3. e_n vs I_C ($V_{CE} = 5 \text{ V}$, $T_A = 25^\circ\text{C}$) for a low-current, high-gain, low-noise bipolar transistor.

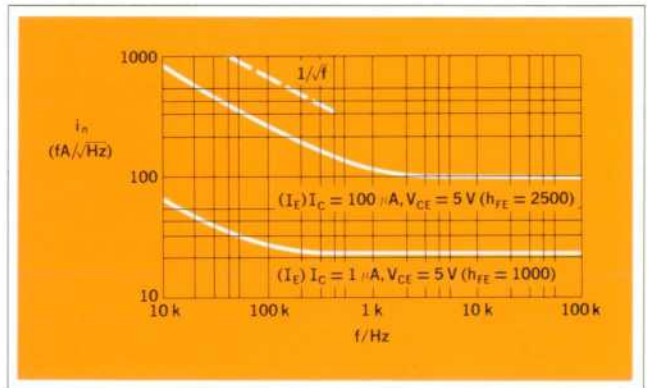


Fig. 4. i_n vs f for $I_C = 1 \mu\text{A}$ and $100 \mu\text{A}$ ($V_{CE} = 5 \text{ V}$) for a low-noise transistor.

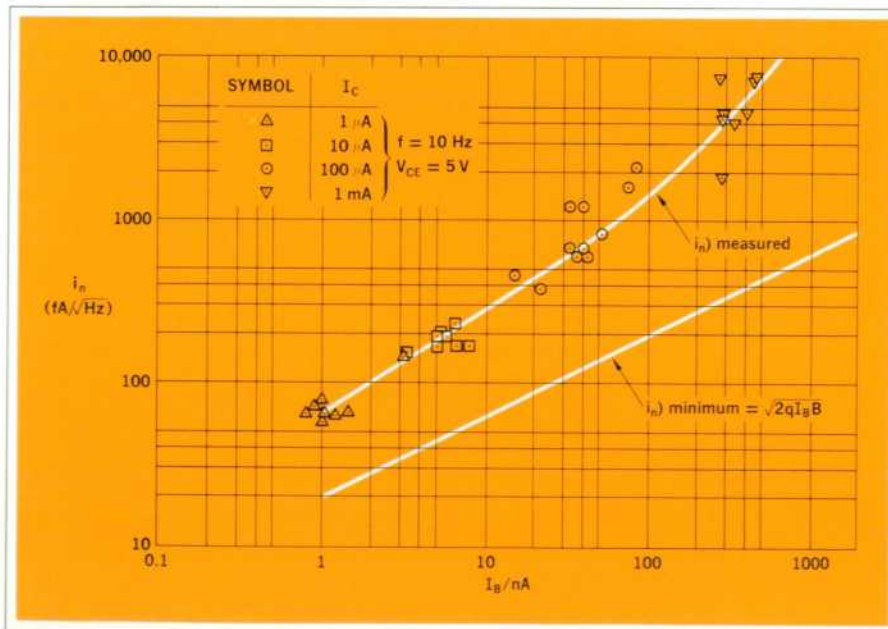


Fig. 5. i_n measured and i_n minimum vs I_B at several values of I_C for a low-noise transistor.

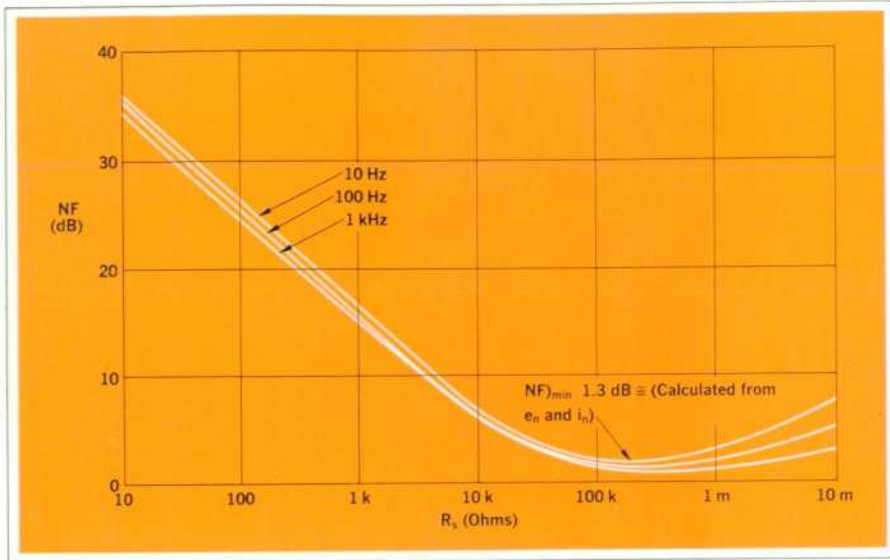


Fig. 6. Noise figure vs R_s at $f = 10$ Hz, 100 Hz and 1 kHz ($I_C = 1 \mu A$, $V_{CE} = 5 V$).

Noise Figure F

From the expression for noise figure shown in the insert of Fig. 2, it may be expected that there is an optimum value of source resistance at which e_n and i_n contribute equally to noise power in R_n and for which the noise figure is a minimum. The experimental data of noise figure at $I_C = 1 \mu A$ vs R_S is shown in Fig. 6 at three frequencies of interest. It can be seen that the noise figure at 10 Hz is less than 3 dB for $R_S = 100 k\Omega$ to 1 M Ω and the calculated minimum is 1.3 dB at a source resistance of about 300 k Ω . Thus, at low currents, the low-current, high gain transistors can be operated from rather high values of source resistance which are comparable to the optimum source resistance of low-noise junction field effect transistors. As I_C is increased, $R_{S\ opt}$

$\left(= \frac{e_n}{i_n} \right)$ decreases and the minimum noise figure increases rapidly. For $f > 1$ kHz, there is very little measurable change in noise figure for collector currents in the range of 1 μA to 100 μA . The noise figure is not very sensitive to the collector-emitter voltage because of the low leakage currents for these planar silicon transistors.

References

- [1]. C. T. Sah, 'Theory of Low-Frequency Generation Noise in Junction-Gate Field Effect Transistors', Proc. IEEE, Vol. 53, pp. 795-814, July 1964.
- [2]. A. S. Grove, Physics and Technology of Semiconductor Devices, ch. 12, p. 334, John Wiley & Sons, 1967.
- [3]. A. L. McWhorter, '1/f Noise and Related Surface Effects in Germanium', M.I.T. Lincoln Lab Report, No. 80, May 1955.
- [4]. S. Christensson, I. Lundstrom and C. Svensson, 'Low Frequency Noise in MOS Transistor, I. Theory, and II.

Experiments', Solid-State Electronics, Vol. 11, pp. 797-820, 1968.

[5]. A. van der Ziel, 'Note on Shot and Partition Noise in Junction Transistors', Journal of Applied Physics, Vol. 25, p. 815, June 1954.

[6]. E. G. Nielsen, 'Behavior of Noise Figure in Junction Transistors', Proc. IRE, Vol. 45, pp. 957-963, July 1957.

[7]. M. C. Swiontek and R. Hassun, 'The Influence of Transistor Parameters on Transistor Noise Performance', Hewlett-Packard Journal, Vol. 16, No. 7, March 1965.

[8]. J. L. Plumb and E. R. Chennette, 'Flicker Noise in Transistors', IEEE Transactions on Electron Devices, Vol. 10, No. 4, pp. 304-308, Sept. 1963.

[9]. W. H. Fonger, 'Noise in Electron Devices', p. 344, ed. by L. D. Smullin and H. A. Haus, Tech. Press of M.I.T. and John Wiley & Sons, 1959.

Nilardi R. Mantena



Neel Mantena, born in Bhimavaram, India, received his B.Sc. degree from Andhra University in 1957, D.M.I.T. from the Madras Institute of Technology in 1960, the M. Tech. degree from the Indian Institute of Technology, Kharagpur in 1961, and the Ph.D. degree in electrical engineering from the University of California, Berkeley in 1966.

From 1961 to 1965 he was a Research Assistant at the University of California working on electron-beam devices and noise reduction in crossed-field microwave amplifiers. Neel joined the Solid State Laboratory of Hewlett-Packard in 1966 and has been concerned with bulk gallium arsenide microwave oscillators, zinc-doped silicon photoconductors, IGFETs and excess noise in solid state devices. He is at present working on a high-gain, low-noise bipolar transistor operating at very low currents, and on a high-power microwave transistor.

Premonitory Heartbeat Patterns Recognized by Electronic Monitor

*Computerlike instrument for intensive care wards provides
advance warning of potentially fatal heart irregularities*

By Thomas C. Horth

BECAUSE A PATIENT MONITORING SYSTEM ALERTS HOSPITAL PERSONNEL to the need for corrective measures while there is yet time, significantly improved recovery rates have been achieved in hospital coronary care units that use these systems.¹ Many lives have been saved because resuscitation was applied within seconds of the onset of life-threatening events, such as cardiac arrest or fibrillation (uncoordinated quivering of the heart muscles)—events that were instantly made known by the equipment.

Experience is showing, however, that it is possible to head off many of these dangerous events, usually by administration of appropriate drugs, if there is some advance warning of their onset. Extensive examination of ECG records has disclosed that the heart gives advance warning in the form of intermittent abnormalities in the ECG waveform, abnormalities which nearly always precede the near-catastrophic events.

Detecting these transient waveform abnormalities, however, poses problems. In the past, nurses have had to constantly monitor ECG waveforms on an oscilloscope, a time-consuming occupation that requires constant attention, difficult to do over long periods of time, and that also keeps trained personnel from performing other duties. What has been needed is an automatic detector that can recognize transient abnormal ECG patterns when they occur and alert medical personnel to the need for action.

A Practical Arrhythmia Monitor

Described here is a practical device, recently developed at Hewlett-Packard, that recognizes the characteristic ECG patterns of these heart abnormalities. What is

more, it keeps track of how often they occur (an occasional abnormal beat is not life-threatening) and it activates alarms if they occur often enough to be considered dangerous. In addition, the instrument accounts for the differences in normal heart beat from person to person and it also recognizes and ignores electrical disturbances arising from muscle movement, electrode slippage, and other interference.

This instrument is called an Arrhythmia Monitor (Hewlett-Packard Model 7822A). It's the central instrument in a system that keeps close watch on the condition of heart patients in the intensive care ward. The complete system includes a standard bedside cardiac monitor, a magnetic tape delay unit, an electrocardiograph, and a trend recorder (Fig. 1). The bedside monitor serves as a preamp for the Arrhythmia Monitor. The electrocardiograph and tape delay work together with the Arrhythmia Monitor to record electrocardiograms of abnormal beats, called ectopic beats by the medical profession. When the Monitor detects an ectopic beat, it directs the electrocardiograph to record the delayed ECG waveform played back by the tape unit, an endless-loop recorder. This arrangement makes it possible to record a few of the heartbeats that precede and follow an ectopic beat, as well as the ectopic beat itself. Over a period of time, the ECG recorder accumulates a relatively compact record that has valuable diagnostic information about the heart's performance.

The trend recorder, a multichannel slow-speed (1 cm/hr) strip-chart recorder, plots an analog record of heart rate and a histogram of number of ectopic beats per minute, information that is supplied in analog form by the Arrhythmia Monitor. This is the first system to provide this kind of information automatically, information that is of high value to the physician as it clearly shows

¹Low, Fakhro, Hood, and Thorn, 'The Coronary Care Unit: New Perspectives and Directions,' *Journal of American Medical Association*, Vol. 199, No. 3, Jan. 15, 1967.

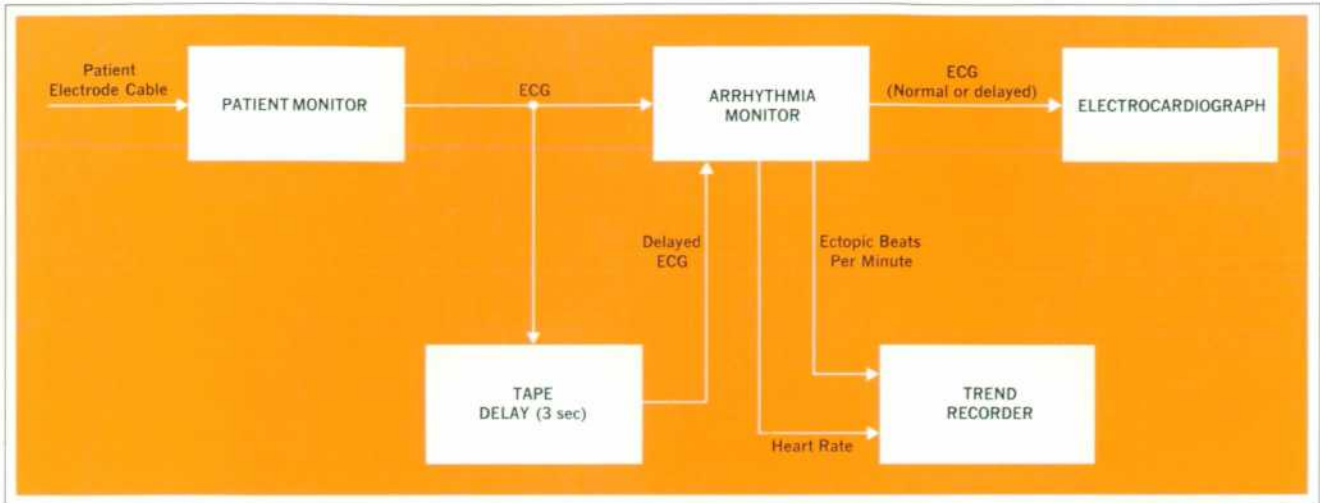


Fig. 1. Patient monitor system that includes Arrhythmia Monitor also has recorders for accumulating important diagnostic information about patient's condition.

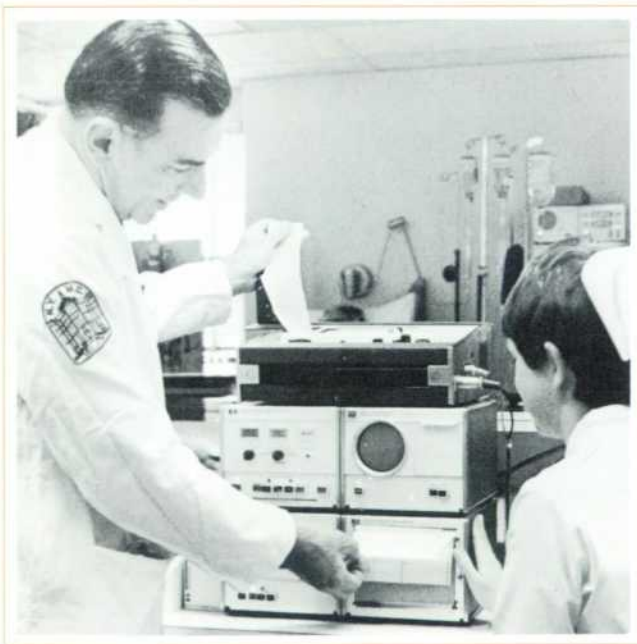


Fig. 2. Arrhythmia Monitor (unit left of oscilloscope monitor) is in compact cabinet that matches other units in Hewlett-Packard Patient Monitor systems.

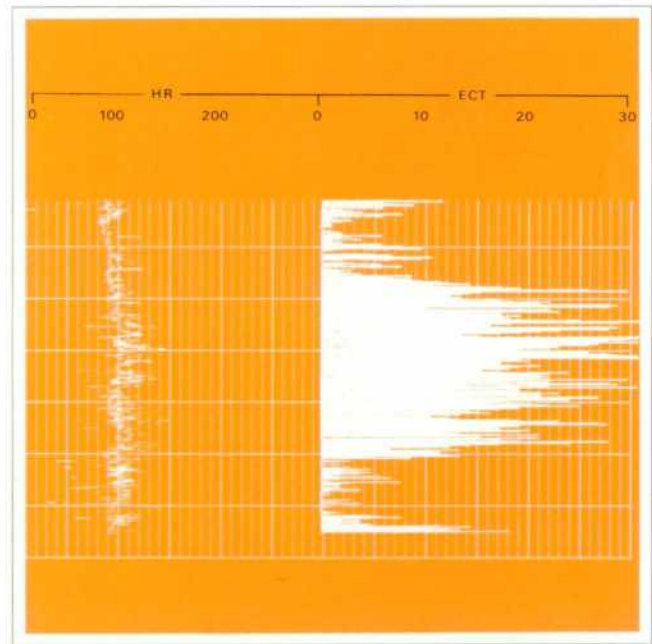


Fig. 3. Trend Recorder plots heart rate (left) and rate of occurrence of ectopic beats over long periods (24 hour record on 24 or 72 cm chart) to show trends in patient's condition.

such things about the patient's progress as how heart rate and heart irritation (number of ectopic beats per minute) responds to drugs (Fig. 3).

This new Arrhythmia Monitor now makes it easier to place the major emphasis in the care of cardiac patients on prevention, rather than resuscitation.

What the Arrhythmia Monitor Looks for

A typical electrocardiogram of a normal heart is shown on the next page. Disturbances in the upper part of the heart—the atria or storage chambers—affect the timing of the heartbeat. The most serious disturbances, though, arise in connection with muscular contractions

Electrical Performance of the Heart

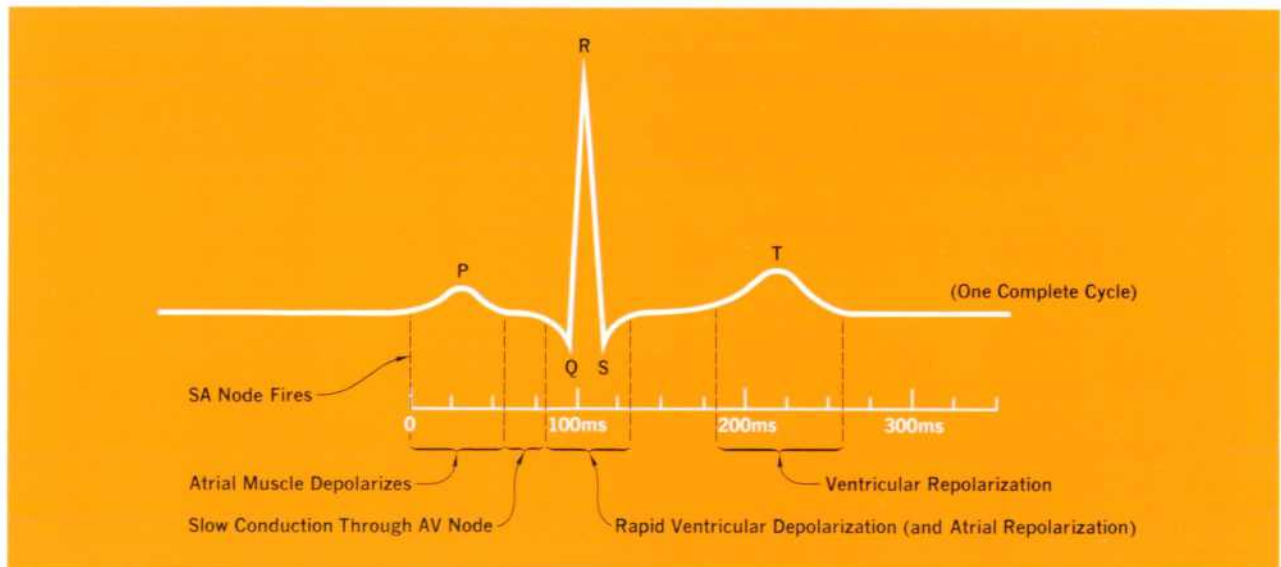
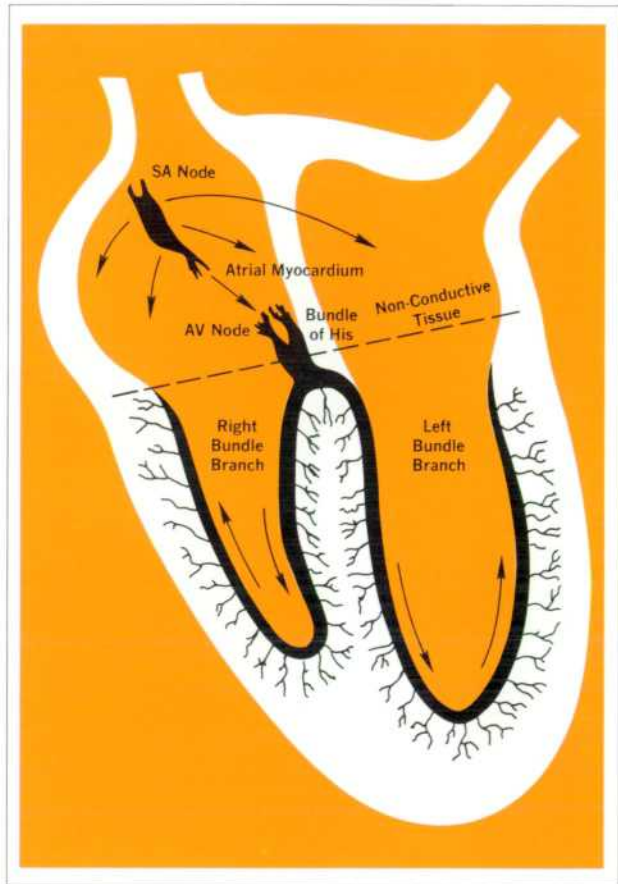
Electrocardiograms are recordings of the heart's time-varying electric fields as sensed by external electrodes. In the normal heart, the beat is triggered by the heart's pacemaker, the sinoatrial node in the upper chambers of the heart. This area is self-triggering tissue that periodically generates electrical pulses normally at 70–80 pulses per second.

The electric field generated by the pacemaker, usually at too low a level to be detected by an electrocardiograph, travels through the muscle cells in the heart's upper chambers (the atria), triggering the atrial muscles into action. The sum total of the resulting muscular electrical activity results in the 'P' wave on the electrocardiogram.

The traveling electrical impulse continues on through the atrioventricular (AV) node, a channel of specialized tissue located at the junction of the walls that separate the chambers of the heart. This tissue—which has a conduction speed of 200 mm/s, about one-fifth that of the atrial walls—conducts the pacemaker pulses to the lower part of the heart. (Other paths from the upper to the lower chambers of the heart are blocked electrically by non-conductive tissue.) Impulse conduction through the AV node is represented by the 'quiet' section between the P and Q waves on the electrocardiogram.

Once past this biological delay line, the pacemaker pulse is spread rapidly over the muscle tissue in the lower part of the heart, the ventricles, by a high-speed conduction system called the Bundle of His. The ventricles are the heart's major pumping muscles and the sum total of their muscular activity is represented on the electrocardiogram by the QRS complex, the most prominent feature of the heartbeat.

Electrical repolarization of the ventricular muscles is represented by the T wave.



of the heart's major pumping chambers, the ventricles. If irritation in the ventricular muscles gives rise to spontaneous activity, the QRS wave is not the sharp, clean spike shown here but is a wider waveform like that shown in Fig. 4.

Heartbeat timing can be affected by many types of disturbances, or arrhythmias, including non-threatening types as well as the serious ventricular ectopic beats. Ventricular ectopic beats are not always displaced in time, though, so timing is not a consistent indicator of ventricular ectopic beats, nor is amplitude. Abnormal width, however, is characteristic of these patterns. Consequently, the Arrhythmia Monitor was designed to look for widened QRS waves, the type of arrhythmia that most often precedes potentially fatal arrhythmias. It also examines heart timing to look for premature beats in those cases where the doctor is interested in disturbances in the atria.

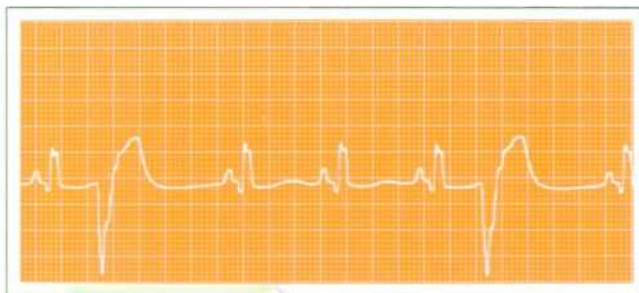


Fig. 4. *Electrocardiogram shows ventricular ectopic beat on 2nd pulse. Arrhythmia Monitor detects abnormal beats like this.*

How It Works

The first task of the Arrhythmia Monitor is to establish what is normal for the patient. It does this when the operator presses the STORE NORMAL pushbutton on the front panel (shown in Fig. 5). For about 4 seconds following momentary depression of the STORE NORMAL pushbutton, the Monitor examines the input ECG waveform and stores values equivalent to the height, width, and derivative of the QRS wave. During this time, the associated ECG recorder is activated to provide visual confirmation that the ECG waveform during this time is indeed normal.

STORE NORMAL signal processing proceeds as follows: the first step is to adjust system gain to normalize waveform amplitude. The input ECG waveform, which may have a peak amplitude anywhere between 0.7 and 3 volts, is first passed through a non-linear slew-rate limiter and a filter (Fig. 6). The slew-rate limiter removes

Ectopic Beats

All of the electrically active tissues in the heart are capable of self-triggering, but at rates slower than the pacemaker. If disease should block the normal conduction paths, the heart can continue to pump blood, but not as effectively as the healthy heart.

When arteries supplying blood to the heart muscles become blocked, the affected muscle suffers from lack of oxygen (ischemia) and ultimately may die (myocardial infarction). The ischemic tissue may become irritated, causing it to 'trigger' on its own. If this occurs in the atria, the atrial muscles may be triggered prematurely. The rest of the heart, though, responds electrically to the premature atrial activity in a normal fashion. Fig. C

If irritation occurs in the ventricles, however, the self-triggering impulse, since it does not arrive through the AV node, travels a different and slower path in spreading over the ventricles. The QRS then becomes widened, and is classified as a ventricular ectopic beat. Fig. D

This kind of interference with the normal electrical performance of the ventricular muscles is the most dangerous, as it may result in ventricular fibrillation (uncoordinated quivering of the ventricular muscles). The new Arrhythmia Monitor detects the occasional widened ventricular beat so that calmatative drugs can be administered before the condition progresses to the dangerous stage.





Fig. 5. Arrhythmia Monitor detects every premature and every widened beat, flashing appropriate indicator lamp (just above row of pushbuttons). Five pushbuttons at lower center select type of beat to be recorded on electrocardiograph. Upper controls select alarm criteria (see Fig. 11).

spikes on the ECG waveform which could not be physiologic in origin, such as electronic pacemaker pulses. The filter has a passband centered at 8 Hz that removes both high- and low-frequency interference.

The filtered waveform is then passed through a full-wave rectifier to make operation independent of ECG signal polarity. The rectified waveform is fed through an automatic gain-controlled amplifier to an amplitude comparator. If the amplitude of any part of the waveform exceeds 1 volt, the comparator reduces the gain of the digitally-controlled AGC circuit by switching in resistors until the signal amplitude no longer exceeds 1 volt. System gain is thus normalized for the ECG waveform of

that particular patient. The system automatically allots 2 seconds for the gain-setting procedure, then it resets the comparator threshold to 400 mV.

The next step is to establish the time of occurrence of each QRS wave. Any subsequent waveform to exceed 400 mV is considered by the comparator to be a QRS wave, provided that 240 ms has passed since the previous QRS. The output of the comparator then triggers a one-shot multivibrator that generates a pulse of standard width and height, which for identification purposes is called the QRS gate. This pulse flashes the front-panel QRS lamp to provide a visual indication of heartbeat occurrence.

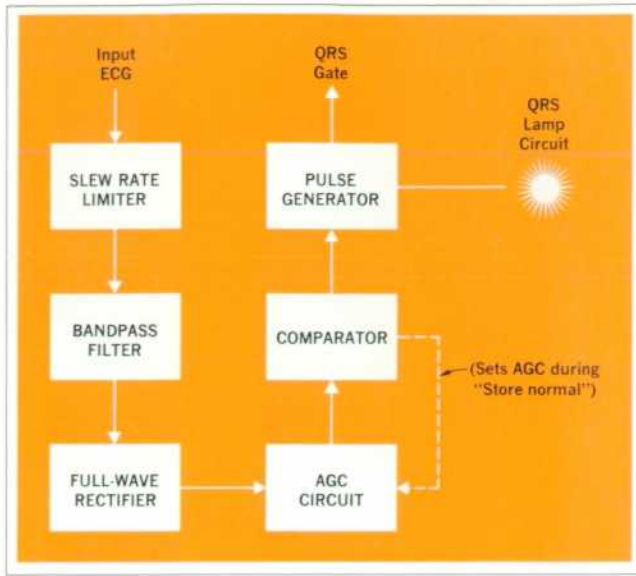


Fig. 6. QRS occurrence detector flashes QRS lamp for every heart beat and generates pulse of standard width and height (QRS gate).

Widened QRS Criterion

To look for widened beats, the Monitor has a second channel, operating in parallel with the QRS detector channel, that senses the beginning and end of the QRS wave (Fig. 7). It does this by examining the derivative of the ECG waveform.

This channel also uses a filter, full-wave rectifier, AGC circuit, and amplitude comparator. This filter, however, takes the derivative of the waveform, as shown in the series of waveforms in Fig. 8. During the STORE NORMAL sequence, the AGC circuit is first set according to the peak value of the differentiated waveform. Following establishment of the AGC level, the comparator's threshold level is reset from 1 V to 200 mV.

The first part of the next waveform to exceed 200 mV turns on a binary if the waveform stays above 200 mV for more than 15 ms. This is considered to be the leading edge of the QRS wave (the 15 ms timing criterion eliminates false counts from noise spikes, electronic pacemaker pulses, or other short-duration interference). The output of this binary passes to another binary that has a turn-off delay of 90 ms, a delay that effectively bridges the separate pulses representing the leading and trailing edges of the QRS complex so that the result is a single pulse (Fig. 8). Finally, a third binary delays the leading edge of the single pulse an additional 75 ms so that the output is a pulse whose duration is equivalent to the width of the QRS complex. This pulse is gated by the QRS gate pulse to remove any between-beat artifacts.

To measure QRS width, the QRS-width pulse operates a gate that allows clock pulses generated at a 167-Hz rate to pass to a totalizer. The count remaining in the totalizer when the gate closes represents the width of the QRS wave. During STORE NORMAL, two more pulses are automatically added to this count to increase the width measurement by 12 ms and the augmented total is then placed in storage.

Width comparison is performed digitally. At the conclusion of each heartbeat, following the STORE NORMAL sequence, the comparator's totalizer is cleared and the stored count placed in the totalizer as a two's complement negative number. The next heartbeat, after being differentiated and rectified, turns on the gate allowing 167-Hz clock pulses to enter the totalizer. Any input that equals or exceeds the stored count causes the totalizer to overflow, which indicates that a widened beat occurred. The overflow flashes the front-panel WIDE indicator (shown just above the WIDE pushbutton in Fig. 5), turns on the ECG recorder if the WIDE pushbutton is depressed, and places a count in another totalizer that keeps track of the number of wide beats.

Premature Criterion

To look for premature beats, the Arrhythmia Monitor compares the time of occurrence of a QRS wave to the time that it should occur as determined by a 4-second running average of QRS occurrences. As shown in Fig. 9, QRS gate pulses are fed to a low-pass filter that produces a dc voltage corresponding to a running 4-second average of the QRS gate pulses, a voltage that is proportional to heart rate ($0-2.4 \text{ V} \propto 0-240 \text{ beats/minute}$). This voltage is made available to the trend recorder for a record of heart rate vs time.

The filter output is also fed to a voltage-to-frequency converter that generates pulses at a rate 2.5 times that of the average heart rate as determined by the filter output. These pulses are fed to a counter.

Both the counter and the V-to-F converter are reset by each QRS gate pulse. If the counter receives two pulses from the V-to-F converter before being reset, that QRS wave is classified as occurring at the normal time. If less than two pulses are counted, however, the R wave is classified as premature. Any R-to-R interval, therefore, that is less than 80% of the average R-to-R interval is classified as premature. The front-panel PRE lamp is flashed, and a count is placed in the register that keeps track of the number of premature beats.

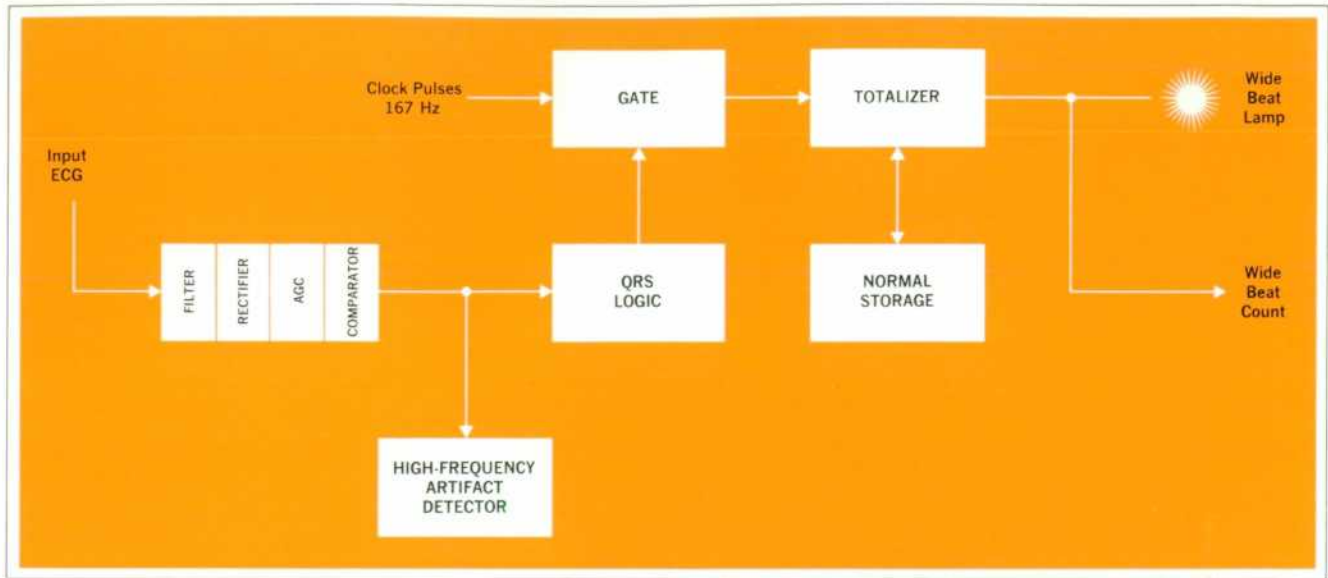


Fig. 7. Widened beat detector makes precision measurement of QRS width by examining derivative of ECG waveform to sense onset and termination of QRS wave.

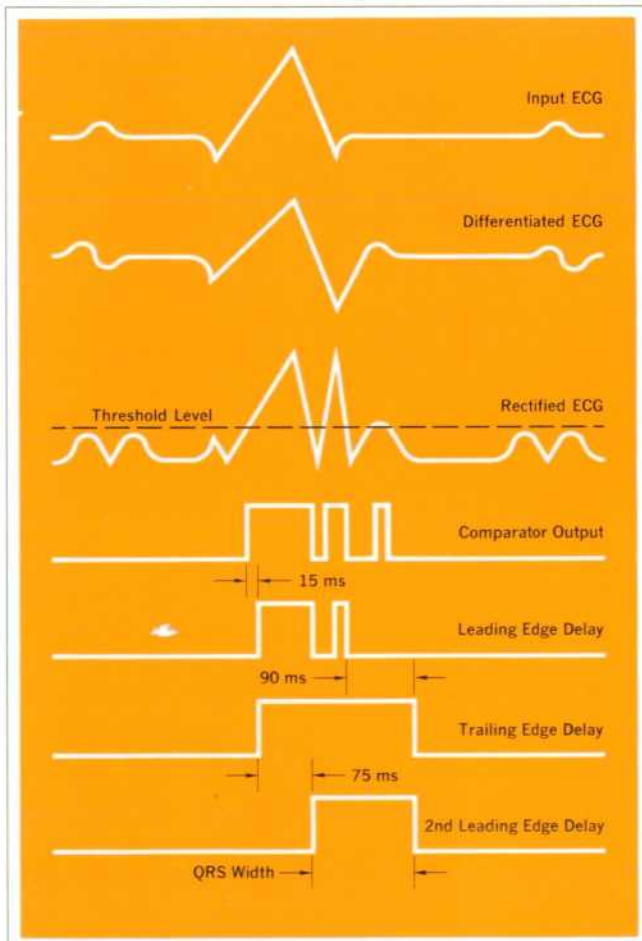


Fig. 8. Waveform processing to measure QRS width.

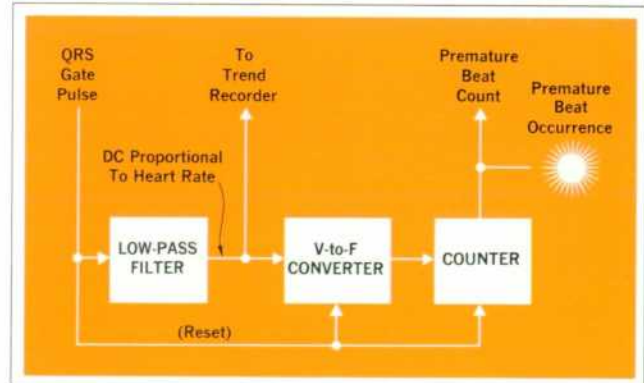


Fig. 9. Premature beat detector compares actual beat occurrence to time that average heart rate indicates beat would be expected.

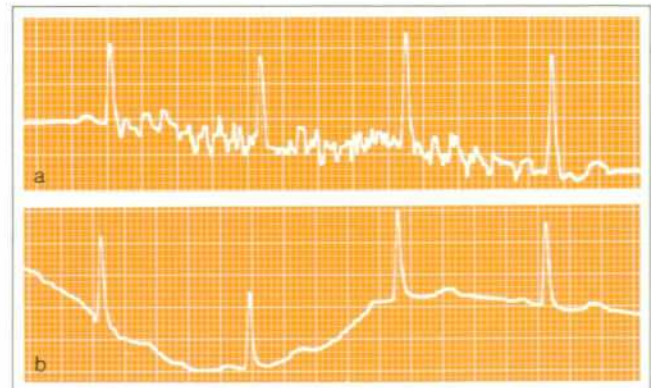


Fig. 10. Muscle activity causes high-frequency interference in ECG (a). Baseline wander is low-frequency noise (b).

This, then, is what the Arrhythmia Monitor does. It examines the width and timing of every QRS wave regardless of how the controls are set. The front-panel controls merely select what the instrument is to do with the resulting information, allowing the system to be tailored to the needs of the particular patient.

Artifact Rejection

Electrocardiograms do not always have the neat appearance illustrated in the box on page 14 but may include interference, called 'artifacts' by the medical profession, like that shown in Fig. 10. These are usually caused by patient muscle movement and/or electrode movement. It is possible that an automatic monitor would classify some artifacts as ectopic beats, so it is important that the Arrhythmia Monitor recognizes artifacts as such.

The two common types of artifact encountered are muscle artifact and baseline 'wander'. Muscle artifact generates a relatively high-frequency noise-like waveform whereas baseline wander is a low-frequency excursion of the ECG waveform. Commonly-encountered amounts of either of these artifacts are reduced to sub-detection levels by the bandpass filters in the width and QRS detector channels.

If muscle artifact is excessive, however, its derivative may exceed the threshold level of the comparator in the width detection channel. A typical muscle artifact crosses the ECG baseline several times in rapid succession so in this case the output of the comparator is a series of pulses. Since the derivative of a genuine QRS wave seldom crosses the baseline more than 4 times, muscle artifacts are detected by a totalizer that counts the number of pulses generated by the comparator during each QRS interval. If more than 5 pulses are counted, the signal is classified as an artifact, the ARTIFACT lamp is flashed, and the ectopic beat indicators are inhibited from classifying the signal as ectopic.

Excessive baseline wander is detected by a third channel, operating in parallel with the width-measurement and timing channels. Here the ECG waveform is passed through a low-pass filter with cut-off at 0.5 Hz, then rectified so negative-going as well as positive-going wander can be detected. The rectified wave is applied to a comparator which is slope sensitive as well as amplitude sensitive—it responds only to signals that exceed 1 V at a rate of more than 667 mV/s. When such a waveform is detected, it too flashes the ARTIFACT lamp and inhibits ectopic beat counting.

By now it should be evident that the instrument uses many logic circuits to perform its duties. Integrated circuits, about 50 of them, have made it possible to cram all these functions at reasonable cost into an instrument of convenient size for bedside use or for mounting with other instruments on a portable cart (price is \$1500). All circuits are contained on just four plug-in circuit cards, allowing quick exchange for servicing.

Instrument Operation

Operating the instrument is simplicity itself. It accepts a high-level ECG-signal supplied by a bedside monitor or suitable preamplifier. The operator confirms operation by noting on a monitor scope that a satisfactory ECG waveform is supplied. Beyond that, the operator selects the alarm criteria and the signals to be recorded—then he presses the STORE NORMAL button. Operation proceeds automatically from then on. The operator need only determine whether or not the ARTIFACT lamp flashes excessively. Operation of the controls is described on a pull-out card, shown in Fig. 11, that is permanently attached to the instrument.

False Counts

Does the Arrhythmia Monitor detect every ectopic beat, and ignore every artifact? It has a high batting average but a realistic appraisal shows that there are some situations where it could be in error. For instance, if patient electrodes are not properly positioned, there may be ectopic beats that have an amplitude less than half the established normal or that have slow rise or fall (low derivative). These won't be counted and may cause the next beat or two to be classified as premature, since the absence of beats affects the averaged R-R interval. Repositioning the ECG electrodes usually corrects this situation.

Large electrical transients may cause a normal beat to appear widened, or may be classified singly as premature beats. Either of these situations would be visible on the ECG recording that results from the instrument's classifying a beat as ectopic.

The Monitor counts all ectopic beats occurring at rates up to 120/minute, but would count every other one if the rate exceeded 120/min. Every ectopic beat at any rate of occurrence, however, is recorded by the ECG recorder.

Field Trials

In hospitals that painstakingly monitor ECG's for early detection, accurate diagnosis, and aggressive treatment of arrhythmias, immediate mortality has been reduced 60%.² A prototype of the new Arrhythmia Monitor, in a year-long trial in a coronary care ward, has shown itself most useful in this effort to inform nurses and attending cardiologists by its ability to make known clinically significant arrhythmias. The instrument and its recorders, by showing the trend of events over periods of time, have shown themselves to be especially useful for assessing the effectiveness of a particular course of drug management. 

Thomas C. Horth

After earning both BSEE and MSEE degrees from MIT plus a BA degree from Oberlin, Tom Horth worked on development of automated air traffic control systems, infrared horizon sensors, and satellite guidance systems. After several years of this activity, curiosity about life styles outside the United States led him to spend the better part of a year with a Norwegian manufacturer of communications equipment. On return to the United States, he



joined the HP Medical Electronics Division (formerly the Sanborn Division) in Waltham, Mass., and worked on the Arrhythmia Monitor, right from the inception of that project. Upon completion of that instrument's development, he applied himself to a study of the application of computers to medical problems.

Tom is married, has two children, does some wood-working in off-hours, and, when time and the weather permit, takes to the New Hampshire hills for skiing.

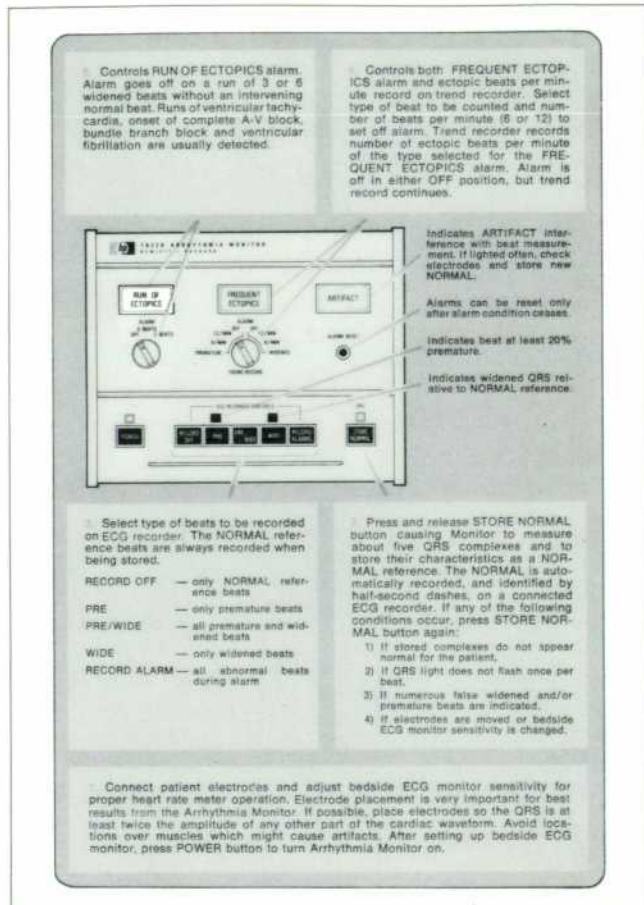


Fig. 11. Slide-out card permanently attached to instrument carries operating instructions.

²Grishman, 'Medical Aspects of Arrhythmia Monitoring,' *Measuring for Medicine*, Vol. 3, No. 5, May-Aug. 1969, Hewlett-Packard Company.